Tunable Magnetic Interaction at the Atomic Scale in Oxide Heterostructures

J. W. Seo,[1,2] W. Prellier,[3] P. Padhan,[3,4] P. Boullay,[3] J.-Y. Kim,[5] Hangil Lee,[5,6] C. D. Batista,[7] I. Martin,[7]
Elbert E. M. Chia,[2] T. Wu,[2] B.-G. Cho,[8] and C. Panagopoulos[1,2,9]

[1]*Cavendish Laboratory, University of Cambridge, Cambridge CB3 0HE, United Kingdom*
[2]*Division of Physics and Applied Physics, Nanyang Technological University, 637371 Singapore*
[3]*Laboratoire CRISMAT, CNRS UMR 6508, ENSICAEN, 14050 Caen Cedex, France*
[4]*Department of Physics, Indian Institute of Technology Madras, Chennai - 600036, India*
[5]*Pohang Accelerator Laboratory, Pohang 790-784, South Korea*
[6]*Department of Chemistry, Sookmyung Women's University, Seoul 140-742, South Korea*
[7]*Theoretical Division, Los Alamos National Laboratory, Los Alamos, New Mexico 87545, USA*
[8]*Department of Physics, Pohang University of Science and Technology (POSTECH), Pohang 790-784, South Korea*
[9]*Department of Physics, University of Crete and FORTH, 71003 Heraklion, Greece*
(Received 20 June 2010; published 14 October 2010)

We report on a systematic study of a number of structurally identical but chemically distinct transition metal oxides in order to determine how the material-specific properties such as the composition and the strain affect the properties at the interface of heterostructures. Our study considers a series of structures containing two layers of ferromagnetic $SrRuO_3$, with antiferromagnetic insulating manganites sandwiched in between. The results demonstrate how to control the strength and relative orientation of interfacial ferromagnetism in correlated electron materials by means of valence state variation and substrate-induced strain, respectively.

The giant magnetoresistance effect in metallic magnetic multilayer systems forms the basis of highly successful magnetic sensing and storage technology [1,2]. The active search for new materials that would allow for ever higher sensitivity and controllability is under way. Transition metal oxides (TMO) are particularly attractive, since there is a plethora of isostructural materials with a wide variety of magnetic and electronic properties, which can be seamlessly built into complex heterostructures [3–10]. In heterostructures composed of different TMO, the disruption introduced even by an ideal interface can drastically upset the delicate balance of the competing interactions among electronic spins, charges, and orbitals, leading to a range of exotic phenomena, including interfacial conduction, magnetism, and superconductivity [3–10]. Among TMO, Mn-based perovskites $AMnO_3$ (manganites) are one of the best studied classes of materials that exhibit a particularly rich set of behaviors tunable by composition, pressure, and temperature [11]. It has been recently demonstrated that when put into contact with ferromagnetic (FM) $SrRuO_3$, the interface layer of antiferromagnetic (AF) manganite becomes FM [12]. In this work we report a strategy and evidence for manipulating the magnetic properties at the atomic level in digitally synthesized nanoheterostructures. We engineer interfacial FM in correlated electron materials by means of valence state variation and substrate-induced strain.

Trilayers, [$SrRuO_3$/manganite/$SrRuO_3$], were grown simultaneously on (001)-oriented $SrTiO_3$ and $LaAlO_3$ substrates using the multitarget pulsed laser deposition technique with energy density of 3 J/cm^2. The conditions for

optimizing the deposition can be found elsewhere [13]. In this study, we chose three types of AF insulating manganites: $CaMnO_3$ with Mn^{4+} (orbital state t_{2g}^3), $Pr_{0.5}Ca_{0.5}MnO_3$ with $Mn^{3+/4+}$, and $PrMnO_3$ with Mn^{3+} ($t_{2g}^3 e_g^1$). The schematic drawing and high resolution electron microscopy (HREM) image of the trilayers [18 unit cell (u.c.) $SrRuO_3$/4 u.c. $Pr_{0.5}Ca_{0.5}MnO_3$/18 u.c. $SrRuO_3$] deposited on $SrTiO_3$ is depicted in Fig. 1(a). HREM was performed on cross-section specimens prepared by mechanical polishing followed by ion milling. The typical HREM image, viewed along the [001] direction [Fig. 1(a)] reveals the epitaxial growth of the trilayers onto the $SrTiO_3$ substrate. Structural characterization of the trilayers with $CaMnO_3$ manganite layer was performed using x-ray diffraction (XRD) [14] and XRD mapping with photon energy of 11 keV as shown in Figs. 1(b) and 1(c). The XRD maps of a reciprocal space in the vicinity of $(hkl) = (103)$ reflection were performed at room temperature at beam line 10 A of the Pohang Accelerator Laboratory in Korea using four-circle diffractometers. The typical twin structure of the $LaAlO_3$ substrate gives rise to the broad peak at (103) [15]. The maps show the in-plane lattices of the substrates and the films match each other without lattice relaxations. The ratio of in-plane to out-of-plane lattice parameters (a/c) estimated by the maps is 0.94 (strong compressive strain) in the case of films grown on $LaAlO_3$ [Fig. 1(b)], whereas $a/c \sim 0.98$ (weak compressive strain) in the case of $SrTiO_3$ [Fig. 1(c)]. The substrate c-axis parameters obtained from $\theta - 2\theta$ scans [the middle panels of (b) and (c)] at the $h = 1$ reflections (guided by the black vertical line on the maps) are 3.789 and 3.906 Å, respectively. An earlier study reports that all the heterostructures we study
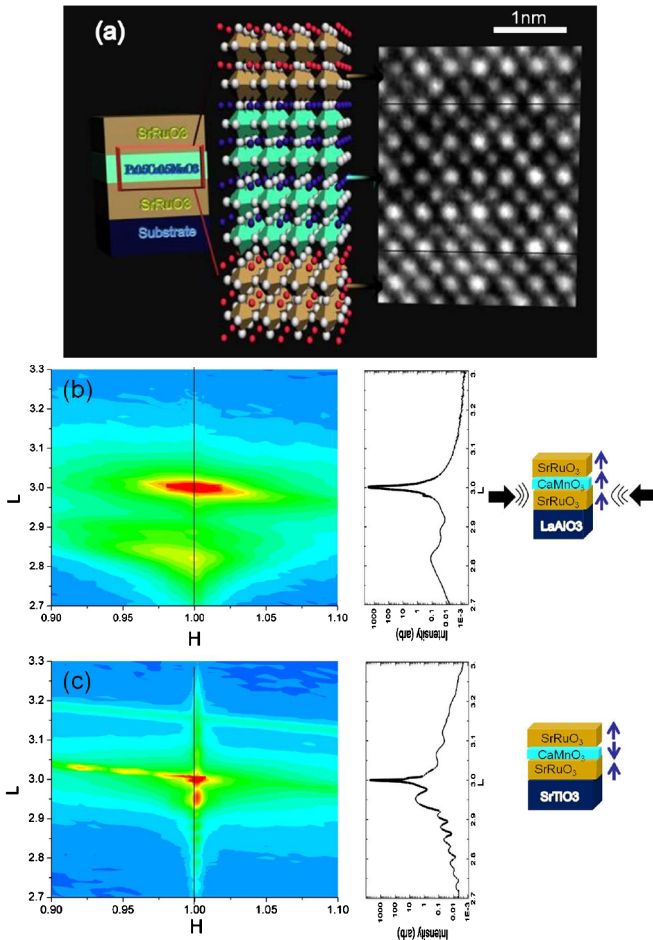
FIG. 1 (color online). (a) Schematic structure (left and middle panels) of the trilayer [18 u.c SrRuO₃/4 u.c Pr₀.₅Ca₀.₅MnO₃/18 u.c SrRuO₃] on SrTiO₃. The high resolution electron microscope (HREM) image (right panel) shows the epitaxial growth of the sample on SrTiO₃. Reciprocal space maps (left panels) of the trilayer [SrRuO₃/CaMnO₃/SrRuO₃] grown on (b) LaAlO₃ and (c) SrTiO₃ near $(hkl) = (103)$. The schematic at the right-hand side of panel (b) depicts the switching or reversal of the spin direction along the c axis due to the effect of strong compressive strain arising from the LaAlO₃ substrate.

here have the same Curie temperature (T_C), i.e., approximately 150 K, close to the T_C of the FM SrRuO₃ film and independent of the substrates and AF spacers [14]. This small variation in T_C indicates the absence of intermixing at the interfaces. The coercive fields measured at 80 K in a magnetic field applied perpendicular to the films (parallel to the easy axis) are 0.2 and 0.5 T for the films grown on SrTiO₃ and LaAlO₃, respectively. The saturated magnetic moments vary from 1 to 1.3 μ_B/unit cell depending on the manganite layers.

We studied the magnetic profile of the manganite layers in the devices using atom-selective x-ray magnetic circular dichroism (XMCD) at the absorption edge of Mn $L_{2,3}$. XMCD measurements were performed at beam line 2A of the Pohang Accelerator Laboratory in Korea. All

XMCD data were obtained after zero-field cooling to 80 K. We measured the total yield signal with an energy resolution of 200 meV in a magnetic field of 0.9 T, perpendicular to the plane of the film. Our approach allows for investigation of a buried layer without spurious signals from neighboring layers or the substrate. The measurement was performed by saturating the magnetization of SrRuO₃ layers in the c direction by a magnetic field in excess of the coercive field. Figure 2 depicts the Mn dichroism spectra ($\rho^+ - \rho^-$), i.e., the difference between x-ray absorption spectroscopy (XAS) data taken with the helicity parallel and antiparallel to the applied magnetic field. The spectra are normalized to the intensity of $\rho^+ + \rho^-$ at the L_3 peak. Notably, Mn dichroism for the samples deposited on LaAlO₃ [Figs. 2(a)–2(c)] has the opposite sign to those grown on SrTiO₃ [Figs. 2(d)–2(f)], implying that the substrate determines the *sign* of the magnetic coupling between Mn and Ru across the interface. The schematic drawings in Fig. 1(b) and 1(c) (right panels) show that the spin direction depends on the substrates the films are grown onto. The large arrows in Fig. 1(b) (right panel) indicate the strong compressive strain is due to the LaAlO₃ substrate.

Table I summarizes the values of the magnetization for the three different manganite layers as deduced from the normalized XMCD, $(\rho^+ - \rho^-)/(\rho^+ + \rho^-)$ (%). In the case of PrMnO₃ grown on the LaAlO₃ substrate, the value of 17% has been estimated to correspond approximately to 1.7 μ_B/Mn determined by the sum rule [16]. The negative sign for the samples grown on SrTiO₃ indicates that the spins of the manganite layer point antiparallel to the applied magnetic field. Notably, the magnetization of the manganite layers deposited on SrTiO₃ is weaker compared
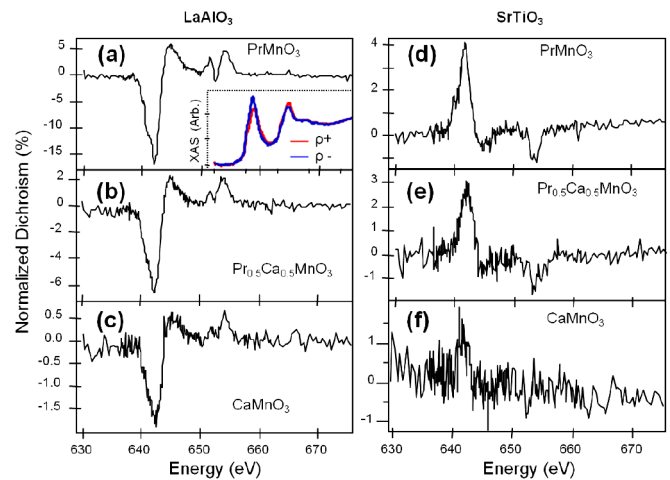

FIG. 2 (color online). Mn $L_{2,3}$ edge XMCD (black: $\rho^+ - \rho^-$) spectra of the manganite layer in the trilayer [SrRuO₃/manganite/SrRuO₃]. Spectra are taken at 80 K in a magnetic field of 0.9 T applied perpendicular to the plane of the film. (a)–(c) and (d)–(f) depict spectra for the samples deposited on LaAlO₃ and SrTiO₃, respectively. Inset in panel (a): Mn $L_{2,3}$ XAS (ρ^+, ρ^-) spectra.

TABLE I.   Magnetization of three types of spacer manganite layers ($CaMnO_3$, $Pr_{0.5}Ca_{0.5}MnO_3$, and $PrMnO_3$) deposited on two different substrates, namely $LaAlO_3$ and $SrTiO_3$. The values of the magnetization are deduced by normalized XMCD signals defined as $(\rho^+ - \rho^-)/(\rho^+ + \rho^-)$.

	$CaMnO_3$	$Pr_{0.5}Ca_{0.5}MnO_3$	$PrMnO_3$
$LaAlO_3$	2%	6.5%	17%
$SrTiO_3$	−1.5%	−3%	−4%

to the heterostructures deposited on $LaAlO_3$. These results indicate that the substrate influences the strength and the direction of the induced magnetization in the manganite layer. Our findings demonstrate that one may be able to prepare tailor-made devices with the desired direction and magnitude of the moment in the nanometer-thin FM interface, by depositing the multilayer on a prespecified substrate. Notably, the observed magnitude of the magnetization follows the order: $PrMnO_3 > Pr_{0.5}Ca_{0.5}MnO_3 > CaMnO_3$, particularly evident for the case of $LaAlO_3$ substrate.

The sign and strength of the interion magnetic exchange interaction is commonly analyzed within the Goodenough-Kanamori (GK) rules [17]. Depending on the orbital occupancy and the presence or absence of an overlap between the orbitals belonging to the two ions, the exchange can be either FM or AF. For instance, for half-filled orbitals with nonzero overlap the exchange is AF [18]. Let us examine what would be the consequences of the GK rules in our system. Ru^{4+} has four electrons in the t_{2g} orbitals. Three of them are ferromagnetically aligned by the onsite Hund's interaction, while the fourth is antialigned with the first three, yielding a state with spin $S = 1$ (the crystal field splitting between e_g and t_{2g} orbitals of Ru exceeds the onsite FM Hund's coupling, which leaves the Ru e_g orbital unoccupied).

In $CaMnO_3$, Mn state is t_{2g}^3 ($S = 3/2$), which corresponds to half-filled t_{2g} band. The Mn atom is connected with Ru via apical oxygen, which leads to one-to-one hybridization between the respective orbitals, e.g., Ru t_{2g} xz (yz) with Mn t_{2g} xz (yz) and Ru e_g $3z^2 - r^2$ with Mn e_g $3z^2 - r^2$ ($z\|$ interface normal). Note that by symmetry, there is no oxygen-mediated hybridization between the xy orbitals of Ru and Mn (we neglect the possible but small symmetry-breaking effects of lattice distortions), while the direct overlap between the orbitals is very weak. The same is true for the $x^2 - y^2$ e_g orbitals. If Ru were in t_{2g}^3 fully polarized state, the GK rules would imply that the coupling between Ru and Mn is AF. However, experimentally we find that on $LaAlO_3$ substrate the coupling is FM. Clearly the FM coupling can only be caused by the fourth—the *minority*—electron of Ru. In the limit of small hybridization between Ru and Mn ions, the sign and magnitude of the magnetic coupling can be understood by means of

perturbation theory in hopping t. The virtual electron hopping processes transfer electrons between low and high-energy ionic sates (the energy difference must be much bigger than t for the perturbation theory to be valid). FM coupling induced by hopping of the minority electron can become dominant if the energy barrier associated with the transfer of this electron between FM aligned Ru to Mn ions is considerably smaller than for the same process for AF alignment of Ru and Mn. We show in the following that there is indeed a significant range of realistic parameters where FM coupling dominates. Whether or not the minority electron contributes to the magnetic coupling between Ru and Mn is determined by the *strain*, which controls the relative energies of the t_{2g} orbitals of Ru. For strong compressive inplane strain, such as the one induced by the $LaAlO_3$ substrate, the xz, yz orbitals are lower than the xy orbital (similarly, e_g $3z^2 - r^2$ is lower than $x^2 - y^2$). These are the orbitals that hybridize across the interface, and therefore when the minority-spin electron of Ru occupies either one of them, it can mediate FM coupling between Ru and Mn. For the tensile strain, however, the minority electron of Ru occupies the xy orbital and does not hybridize with Mn, which leaves only the AF channel open.

To test this qualitative argument, we performed exact diagonalization studies of the $Mn^{4+} - Ru^{4+}$ complex including all d orbitals for various values of effective Ru-Mn hopping integral t and strain-induced crystal field splitting, $\delta = \varepsilon_{xy} - \varepsilon_{xz,yz}$ (Fig. 3). The hopping integral is taken to be zero between the d orbitals for which by symmetry there is no oxygen-mediated hybridization (xy case). The spin state of isolated Mn ion is $S_{Mn} = 3/2$ and of isolated Ru ion is $S_{Ru} = 1$. The Hamiltonian is

$$H_0 = \sum_{j,\alpha} \varepsilon_j n_{j\alpha} + \sum_{j,\alpha} U_j n_{j\alpha\uparrow} n_{j\alpha\downarrow} + \sum_{j,\alpha \neq \alpha'} \frac{U_j - J_j}{2} n_{j\alpha} n_{j\alpha'}$$
$$- \sum_{j,\alpha \neq \alpha'} \frac{J_j}{2}\Big[\mathbf{S}_{j\alpha} \cdot \mathbf{S}_{j\alpha'} + \frac{1}{4} n_{j\alpha} n_{j\alpha'} - d^\dagger_{j\alpha\uparrow} d^\dagger_{j\alpha\downarrow} d_{j\alpha'\downarrow} d_{j\alpha'\uparrow} \Big]$$
$$+ \delta \sum_j (n_{jxz} + n_{jyz}) + \sum_{\alpha,\alpha',\sigma} t_{\alpha\alpha'} (d^\dagger_{1\alpha\sigma} d_{2\alpha'\sigma} + \text{H.c.}), \quad (1)$$

where $j = Mn^{4+}, Ru^{4+}$, U_j are the Coulomb repulsions and J_j are the Hund's coupling constants. The orbital label α takes the values $\alpha = \{xy, xz, yz\}$, while $\sigma = \uparrow, \downarrow$ is the spin label. Finally, $n_{j\alpha\sigma} = d^\dagger_{j\alpha\sigma} d_{j\alpha\sigma}$ and $n_{j\alpha} = \sum_\sigma n_{j\alpha\sigma}$. The hopping matrix is diagonal, $t_{\alpha,\alpha'} = t_{\alpha,\alpha} \delta_{\alpha,\alpha'}$, with $t_{xy,xy} = 0$, $t_{xz,xz} = t_{yz,yz} = t$. We use parameters [19] $J_{Ru} = J_{Mn} = 1.5$ eV, $U_{Mn} = 5$ eV, $U_{Ru} = 4$ eV, $\varepsilon_{Mn} - \varepsilon_{Ru} = -2$ eV. We find that for $\delta \gtrsim \delta_c(t)$ (strong compressive strain) where $\delta_c(t)$ is a critical value of δ, the sates with high total spin ($S_{tot} = 5/2$ and $S_{tot} = 3/2$), are stabilized, which corresponds to FM coupling between Mn and Ru. The critical value of δ for the transition between $S_{tot} = 1/2$ and $S_{tot} = 3/2$ depends on the value
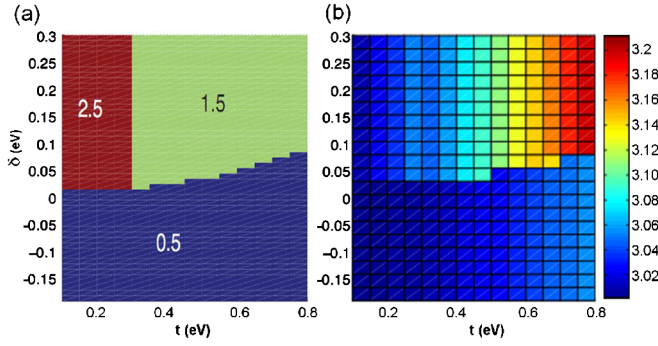
FIG. 3 (color online).   (a) The total spin of coupled Mn^{4+} ($S = 3/2$) and Ru^{4+} ($S = 1$) as a function of interion t_{2g} hybridization t and the crystal field splitting $\delta = \varepsilon_{xy} - \varepsilon_{xz,yz}$. (b) The charge of the Mn ion. The transitions between different total spin states are accompanied by the change in the charge of the ions.

of t [see Fig. 3(a)]. We point out that the state with $S_{\text{tot}} = 3/2$ that appears at larger values of hopping t is beyond the ionic picture. On the other hand, for $\delta < \delta_c(t)$ (tensile or weak compressive strain) the Ru and Mn ions are antialigned into the state with lowest total spin ($S_{\text{tot}} = 1/2$). This is in agreement with the above qualitative discussion.

In $PrMnO_3$, the nominal valence of Mn is $3 +$; i.e., there is one extra electron in the e_g orbital of Mn. Because of the Hund coupling, the spin of this electron is aligned with the spins of the other (t_{2g}) electrons of Mn. In the case of strong compressive inplane strain ($LaAlO_3$ substrate) the extra e_g electron occupies the $3z^2 - r^2$ orbital of Mn, which is well hybridized with the corresponding empty orbital of Ru, and therefore according to the GK rules favors FM alignment of Mn and Ru spins. This contribution adds to the FM coupling that is already present in the case of $CaMnO_3/SrRuO_3$ interface. In addition, the magnetic moment is bigger for the Mn^{3+} ion ($S_{Mn} = 2$). Both effects lead to the relatively enhanced value of the induced FM moment in $Pr_{0.5}Ca_{0.5}MnO_3$ and $PrMnO_3$, in agreement with the progression that we observe experimentally (Table I). On the other hand, for tensile or weak compressive inplane strain ($SrTiO_3$ substrate), the extra electron on Mn occupies the e_g $x^2 - y^2$ orbital, which by symmetry cannot hybridize with the apical oxygen orbitals and thus does not have significant overlap with the Ru d orbitals across the interface. Thus we conclude that for tensile or weak compressive inplane strain, just as in the case of $CaMnO_3$, in $Pr_{0.5}Ca_{0.5}MnO_3$ and $PrMnO_3$, there is no virtual hopping process that would favor FM alignment of Mn and Ru ions, and the result is a (relatively weak) AF coupling between Mn and Ru ions. This is in complete qualitative agreement with our experimental observations.

In summary, we report direct evidence for tunable FM behavior at the atomic scale in strongly correlated oxide heterostructures. We find that the orientation and strength of the induced interfacial magnetism can be very sensitive to strain. By selecting appropriate substrate one may now design complex magnetic heterostructures with the desired relative arrangement of the magnetic elements, of potential utility to electronics and spintronics, including magnetic memory and sensing. Moreover, the strain can be also induced by means of externally applied force, which can thus cause mechanically induced magnetic reorientation. For example, by using a piezoelectric substrate such as PNM-PT ($Pb(Mg_{1/3}Nb_{2/3})O_3 - PbTiO_3$) [20] one would be able to control the orientation and strength of the magnetization by tuning the lattice parameters by means of an applied electric field.

[1] G. Binasch, P. Grünberg, F. Saurenbach, and W. Zinn, Phys. Rev. B **39**, 4828 (1989).
[2] M. N. Baibich et al., Phys. Rev. Lett. **61**, 2472 (1988).
[3] Y. Tokura and N. Nagaosa, Science **288**, 462 (2000).
[4] A. Ohtomo and H. Y. Hwang, Nature (London) **427**, 423 (2004).
[5] A. Brinkman et al., Nature Mater. **6**, 493 (2007).
[6] A. Gozar et al., Nature (London) **455**, 782 (2008).
[7] S. Thiel, G. Hammerl, A. Schmehl, C. W. Schneider, and J. Mannhart, Science **313**, 1942 (2006).
[8] J. Heber, Nature (London) **459**, 28 (2009).
[9] G. Logvenov, A. Gozar, and I. Bozovic, Science **326**, 699 (2009).
[10] J. Mannhart and D. G. Schlom, Science **327**, 1607 (2010).
[11] Y. Tokura, Colossal Magnetoresistive Oxides Advances in Condensed Matter Science (Gordon and Breach Science Publishers, Amsterdam, 2000), Vol. 2.
[12] Y. Choi et al., Appl. Phys. Lett. **91**, 022503 (2007).
[13] P. Padhan, W. Prellier, and B. Mercey, Phys. Rev. B **70**, 184419 (2004).
[14] P. Padhan and W. Prellier, Phys. Rev. B **76**, 024427 (2007).
[15] C. Aruta et al., J. Appl. Phys. **100**, 023910 (2006).
[16] C. T. Chen et al., Phys. Rev. Lett. **75**, 152 (1995).
[17] J. Kanamori, Prog. Theor. Phys. **17**, 177 (1957); J. B. Goodenough, J. Phys. Chem. Solids **6**, 287 (1958).
[18] P. W. Anderson, Phys. Rev. **79**, 350 (1950).
[19] J. M. D. Coey, M. Viret, and S. Von. Molnar, Adv. Phys. **48**, 167 (1999).
[20] O. Bilani-Zeneli et al., J. Appl. Phys. **104**, 054108 (2008).